Two phase flow in porous media with and without seismic stimulation

Mihailo Jankov

Thesis submitted for the degree of Ph.D.

Department of Physics
University of Oslo, Norway

March 2010

Series of dissertations submitted to the
Faculty of Mathematics and Natural Sciences, University of Oslo
No. 936

ISSN 1501-7710

Cover: Inger Sandved Anfinsen.
Printed in Norway: AiT e-dit AS.

Produced in co-operation with Unipub.
The thesis is produced by Unipub merely in connection with the
thesis defence. Kindly direct all inquiries regarding the thesis to the copyright
holder or the unit which grants the doctorate.

To Mileva Jankov

Preface

This thesis summarizes the work I did in the last three years as a member of the Advanced Materials and Complex Systems (AMCS) group at the University of Oslo (UiO) in the fascinating world of flow in porous media. Working with my fellow AMCS group members was an unforgettable experience in both scientific and non-scientific sense. I am taking this opportunity to express my gratefulness to the people who introduced me to this wonderful environment and a whole new field. It took some courage to employ a meteorologist as an experimentalist in a group that investigates flow in porous materials. First and foremost I want to sincerely thank my academic adviser Professor Knut Jørgen Måløy for taking me as a graduate student and guiding me on my way to the doctoral degree. As my principal advisor he has been there whenever I needed help or advise. I also want to thank my co-adviser Professor Eirik Grude Flekkøy for showing the same dedication and belief in my success within the group and the project. A huge deal of my success is due to the help of the people from the mechanical workshop. They helped with designing the experimental apparatus and providing good solutions in timely fashion. Finally, this work would have been impossible to carry out without a substantial funding coming from the Norwegian Research Council (NRC) and the PETROMAKS project grant. My academic advisers along with the Institute for Physics at UiO provided additional funding that largely helped in the completion of the thesis and the doctoral degree.

The social environment and the general atmosphere in the group made my work on the project even more enjoyable. I want to thank Grunde, Henning, Olav, Michael, Stephane, Ken Tore, Jan Ludvig, Vitaly, Jørn Inge, Bjørnar, Pop, Joachim, Mark and Mateusz for the great time we had not only working together but also socializing. I especially want to acknowledge the help I received from my friend and colleague René Castberg. He was someone who knew where the solutions for my computational problems were in those rare moments when he could not provide them himself.

One of the great things about the AMCS group is its openness to the collaboration with other groups and people. Over the course of my Ph.D track I met Professor Renaud Toussaint from Institut de Physique du Globe de Strasbourg in France and Ramon Planet from Departament d'Estructura i Constituents de la Matèria in Barecelona, Spain. Knowing them and working with them also made my work more enjoyable enriching

my overall experience.

Finally, I must acknowledge people who have always been a great support and motivation not only during my Ph.D program but in my day to day life. I thank my family, Marion, Isidor and Milla as well as my father Nikola and sister Isidora for everything they have done to make my life easier while striving to achieve my academic goals.

Oslo, December 2009
Mihailo Jankov

Contents

List of Papers

Paper 1 Løvoll, G., Jankov, M., Måløy, K. J., Toussaint, R., Schmittbuhl, J. and Schäfer, G.: *Influence of viscous fingering on dynamic saturation–pressure curves in porous media*
Submitted to Transport in Porous Media

Paper 2 Jankov, M., Løvoll, G., Knudsen, H. A., Måløy, K. J., Planet, R., Toussaint, R. and Flekkøy E. G.: *Effects of pressure oscillations on drainage in an elastic porous medium*
Published in Transport in Porous Media:DOI 10.1007/s11242-009-9521-z

Paper 3 Jankov, M., Løvoll, G., Måløy, K. J., Knudsen, H. A., Aursjø, O. and Flekkøy E. G.: *Vibrational stimulation of a slow drainage flow*
Preprint

1 Introduction

This thesis is focused on the investigation of multiphase fluid flow in porous media. Historically, studies on fluid behavior in different porous materials have drawn a lot of attention due to their appeal and practical value in various fields of human activity. The applicability of this sort of research ranges from the fields like medicine, civil engineering, hydrology, hydrogeology and environmental engineering to the petroleum industry.

More specifically, the motivation for this study comes from a need to better understand how slow moving fluids behave in a reservoir under different externally imposed boundary conditions. In not so distant past numerous reports on enhanced oil recovery after seismic activity [1, 2] started to intrigue the oil community. The interest in knowing what really happens in the reservoir affected by a seismic episode soon became of importance for the scientific community too. Here, we are investigating the physics behind the slow non-stimulated and stimulated flow. The work presented in the thesis is of experimental nature. All the experiments are performed on a synthetic porous medium created in the laboratory.

Porous systems are disordered and studying the flow through such a complex system is a complex task. Coupling different sorts of fluids and a porous system can lead to many different scenarios in terms of flow regimes depending on the intrinsic properties of the fluid and the medium. The work in this thesis addresses the pore scale effects of externally imposed forcing on the multiphase flow. These effects consequently have different repercussions on the invading cluster geometry. A thorough discussion of the fluid and porous matrix properties along with the resulting flow is given in the following paragraphs.

There are three objectives, therefore three segments that are interconnected to a large degree. Here, the impact of viscous forces on the so-called dynamic capillary pressure [3] and on the global saturation of the medium with the non-wetting fluid is investigated first. As a result in this part we propose a scaling relation between the measured capillary pressure and the saturation of the medium with the non-wetting fluid. These results can potentially be implemented in reservoir modeling. The interest is then shifted to the effects of pseudo-seismic stimulations on the fluid flow and the resulting invading cluster geometry. The flow is stimulated by two different methods that mimic seismic events and the results of that stimulation are then investigated. The first method consid-

ers pressure oscillations applied to the non-wetting phase in a slow drainage flow. Different combinations of the oscillatory pressure amplitudes and frequencies differently affect the flow regime and therefore the invading cluster morphology. By proposing a dimensionless number we manage to successfully categorize the resulting geometries and the respective flow regimes. We also stimulate the flow by means of oscillatory displacement of the entire porous matrix in the horizontal plane while the wetting fluid is drained out of the medium. The effects of the displacement in the direction of and in the direction perpendicular to the flow are monitored and the results are reported.

The organization of the thesis is as following. The second chapter covers the delineation of the experimental setup. In the first part an elaborate description of the synthetic porous matrix and the apparatuses that are used for the pseudo-seismic stimulation is given. Simply said, the porous medium used here is a monolayer of glass beads sandwiched between a plexiglass plate on the top and a 'water-' or 'air-cushion' on the bottom. The term porous matrix in the further text will be interchangeably used with the term model or porous model. One of the goals in the construction of the porous matrix was to create a structure that would represent a real world system. The fidelity of this representation is achieved to a fairly high degree. Here, the reader is presented with how well the synthetic model depicts a reservoir material in terms of compressibility (elasticity), porosity and permeability. The characteristics of the synthetic porous medium are then put in the perspective of a real reservoir and a comparison with an imaginable scenario is presented. In this segment we also want to draw the reader's attention to the importance of the elasticity of the model and its effect on the flow regime.

A brief theoretical background of a drainage process on the pore scale is given in the third chapter of the thesis. The basic principles and the governing forces of non-stimulated drainage are presented. This chapter covers the definitions of the terms widely used through the thesis as well. Here, the reader gets familiarized with some of the effects that the flow speed, viscosity and density contrast as well as the gravitational force have on the geometrical properties of the invading cluster and the flow regime. The effects of pseudo-seismic stimulation on slow drainage are introduced in the second part of this chapter. We look into how the flow and the invading cluster morphology are altered when stimulated by means of either oscillating pressure in one of the phases or a physical displacement of the entire porous matrix in the horizontal plane.

The final chapter gives a brief introduction of the scientific papers that constitute the thesis. There are three papers and all of them report the results achieved through experimental work. The papers are not ordered in a chronological fashion but rather in a way which introduces the reader to the general problem of quasi two-dimensional flow first and then later on points to a possibility to alter and control the flow regime by using various methods to stimulate the flow.

2 Experimental setup and procedures

In this chapter three experimental setups are described. The specific details of each setup are given after the common element found in all of them is depicted. The core piece of the setup is the porous matrix. The porous matrix is always prepared in the same way. The only difference from one experiment to another is the size of the porous model In the case when the non-stimulated and the oscillatory pressure driven flow are studied the size of the matrix is larger than that used in the experiments where the matrix is shaken in the horizontal plane.

2.1 Porous matrix

The quasi two-dimensional synthetic porous medium consists of a monolayer of 1 mm diameter glass beads between two sheets of transparent contact paper. To create the matrix, a sheet of contact paper is attached to a plexiglas plate. The adhesive side of the contact paper is then covered with the beads leaving a randomly distributed monolayer across the entire area. Two openings aligned with the inlet and outlet channels on the plexiglas plate are made. To prevent the uncontrolled outflow of the fluid and to outline the active area of the porous matrix silicon glue is used. After the silicon glue is applied the matrix is closed by adhering another sheet of contact paper to the beads. The plexiglas plate is then turned and attached to either a 'water-' or a pressurized 'air-cushion' depending on the sort of the experiments it is prepared for. The porous matrix is secured between the plexiglas plate and the pressure-cushion. One of the purposes of the cushion is to prevent horizontal motion of the beads. By circulating temperature controlled water through the water cushion the effect of the change in room temperature on the fluid viscosity can be minimized. A schematic view of the porous model is given in Figure 2.1.

The dimensions of the porous model and the active matrix vary from experiment to experiment. Generally, when the non-stimulated flow is studied as well as in the case of the oscillatory pressure experiments, the model size is 50 cm $\times$ 50 cm, with the active matrix of 35 cm $\times$ 20 cm $\times$ 0.1 cm. Needing to reduce the weight of the porous model due to the limitations of the experimental setup when the flow undergoes vibrational stimulation we use a 30 cm $\times$ 30 cm large model. The active matrix in the latter case is

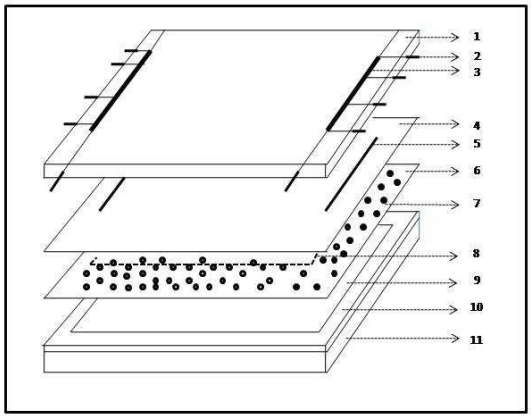

Figure 2.1: *Schematic view of the porous model: 1-upper Plexiglas plate, 2-inlet/outlet tubing connector, 3-inlet/outlet channel, 4-upper adhesive paper sheet, 5- slit, 6-lower adhesive sheet, 7-monolayer of glass beads, 8-silicone filling (defines the geometry of the active matrix), 9-mylar film, 10-aluminum rim and 11-lower Plexiglas plate. Elements 9, 10 and 11 define the pressure cushion.*

17 cm $\times$ 10 cm $\times$ 0.1 cm. The porous matrix permeability is κ=1.9×10^{-5} cm^2 and the porosity is ϕ_0=0.63. The volume of a single pore is approximately 1 mm^3.

2.1.1 Non-stimulated drainage

Because of different needs in each experiment the mechanisms to drive the fluids through the matrix or to stimulate the flow are experiment specific. In the non-stimulated flow experiments the wetting fluid is extracted from the porous matrix in two ways. First a set of experiments in which the pressure difference between the fluids is created by means of the hydrostatic pressure change is performed. An open container with the wetting fluid is placed on an electronic scale that rests on a translation stage. The container is connected to the matrix through the tubing system. Moving the translation stage upwards or downwards relative to the porous matrix causes a positive or negative change in the hydrostatic pressure. The hydrostatic pressure difference between the container and the matrix drives the wetting fluid flow in or out from the porous system. The change of the fluid mass in the open container is measured on the scale.

The flow through the porous matrix can also be initiated and maintained by the use of a syringe pump. When a syringe pump is used, the outflow rate is set to be constant.

These two methods of driving the fluid through the medium are completely different in terms of how the fluid flow is maintained. Using the translation stage, we lower the open container slowly in small height increments. In each of these steps, the pressure

difference between the fluids is increased. The whole process is very slow and basically quasi-static. On the contrary, when the syringe pump is used, the flow rate is set to a constant value. This means that the pressure in the fluids constantly readjusts itself to maintain the constant flow rate. This method is preferable when there is a need of having a good control of the flow velocity.

The porous model is transparent and the used fluids are in contrasting colors. By placing the matrix above a light source we are able to take pictures of the evolving invading cluster. The pressure in both fluids is monitored and read off the pressure sensors. The pressure sensors reside on the inlet and outlet channel. The information from the sensors is acquired and then transfered to a PC through a data acquisition card. This experimental setup is shown in Figure 2.2.

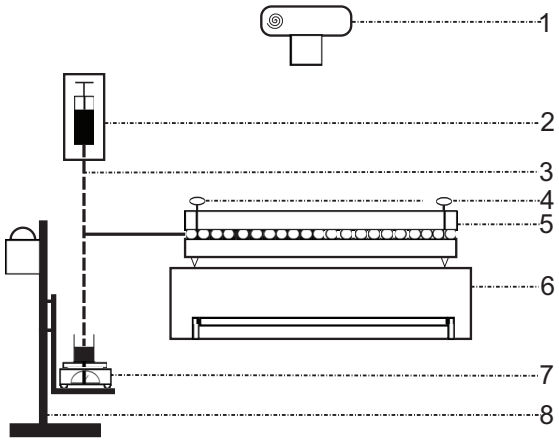

Figure 2.2: *Schematic view of the experimental setup 1: 1-digital camera, 2-syringe pump 3-tubing system, 4-pressure sensors, 5-porous model (connected to either the syringe or gravitational pump through the tubing system, 6-light box with fluorescent lighting, 7-electronic scale, 8-translation stage operated by a step motor.*

The experiments start by imposing the pressure difference across the fluid interface either by the gravitational or the syringe pump. The amount of displaced fluid is measured and combined with the duration time of the experiment to give the temporal evolution of the matrix saturation. The pressure time evolution during the experiment is also recorded. Combining the pressure and saturation data so-called pressure saturation curves are plotted. These experiments are performed for different outflow rates, therefore we are able to study the impact of the flow velocity on the pressure-saturation curves.

2.1.2 Mechanisms of seismic stimulation

To simulate a seismic event we devise two methods. Firstly, pressure oscillations by using a custom made air pump are applied to the non-wetting phase. The pump is constructed as a cylinder with a piston inside. The cylinder has two openings, a pinhole sized air inlet and an outlet. The outlet is attached to the porous matrix. The forward and backward motion of the DC motor operated piston expands and compresses the air in the chamber creating oscillations in the air pressure at the inlet of the porous model. The frequency of the oscillations corresponds to the frequency of the piston. The amplitude of the oscillations is tunable and can be adjusted by changing the volume of the chamber. On average the air pressure is equal to the atmospheric pressure in the laboratory. To initiate and maintain the flow of the wetting fluid out of the matrix a syringe pump is attached to the model outlet. A schematic view of the complete model setup is shown in Figure 2.3.

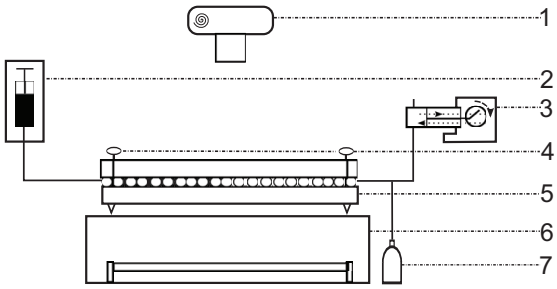

Figure 2.3: *Schematic view of the experimental setup 2: 1-camera, 2-syringe pump, 3-DC motor operated air pump, 4-pressure sensors, 5-porous model (connected to the syringe and air pump through a system of tubings, 6-light box with fluorescent lighting, 7- air container of variable volume.*

The other method to simulate effects of a seismic event on the flow in the porous cell is to place the cell in a specially constructed frame that can be displaced in the horizontal plane. A commercially available shaker moves the frame back and forth at a given frequency and acceleration amplitude. As in the previous cases the frame with the porous cell is placed on a light box. The wetting phase is slowly removed from the matrix as the cell is set in motion. The development of the invading cluster is captured by a digital camera placed over the porous model. To control the acceleration of the shaking motion an accelerometer is attached to the porous matrix. The data from the accelerometer are read off by a data acquisition card and sent to the PC. An overview of the main elements of the apparatus is shown in Figure 2.4.

Initially the matrix is saturated with the incompressible wetting fluid in both cases. The defending, wetting fluid, is withdrawn from the medium at a low, constant outflow rate (Q=0.022 and Q=0.06 ml/min for oscillatory and shaking stimulation, re-

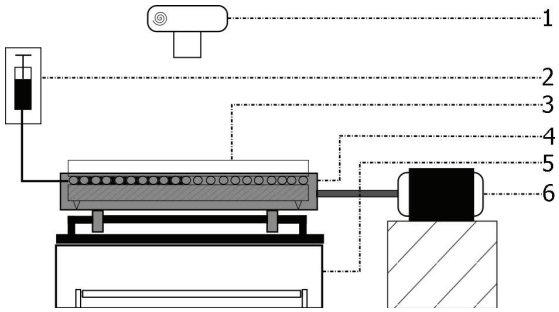

Figure 2.4: *Schematic view of the experimental setup 3: 1-camera, 2-syringe pump. 3-porous model, 4-aluminum frame, 5-commercial shaker on the mount, 6-light box with fluorescent lighting.*

spectively). Essentially the background flow is kept in the capillary regime while either the pressure oscillations or the vibrational stimulation is applied. The images of the evolving invading pattern are taken in even time intervals and stored on the PC. The experiment ends immediately before breakthrough, the moment invading clusters reach the outlet channel.

3 Non-stimulated and stimulated pore scale drainage process

Firstly, the physics behind the slow, non-stimulated quasi two-dimensional drainage is elaborated. This segment gives an overview of the basic forces on the pore scale and their effects on the flow. After the most essential aspects of two-phase flow are presented the reader will be introduced to the physics and consequences of seismically stimulated flow. Before getting into details, since the work summarized in this thesis is exclusively focused on drainage, the term drainage is going to be explained first. In the case when the fluids used in a two-phase flow are different with respect to their wetting properties, depending on which phase is the defender and which one is the invader the flow can be categorized as imbibition or drainage. The interface between the fluids is called front. The direction of the flow is controlled by the pressure difference between the phases. If the pressure in the non-wetting phase is larger than that in the wetting phase the front will be moving towards the wetting phase and vice versa. The situation in which the wetting phase is displaced by the non-wetting phase is known as drainage, otherwise it is called imbibition. Fluids can be separated on wettable or non-wettable based on the angle θ the interface between them builds when in contact with a flat surface. For a θ greater than 90 degrees the non-wettability condition is met. On the contrary, if the created angle is less than 90 degrees, the fluid is considered to be wettable. A schematic view of the wetting angle is shown in Figure 3.1.

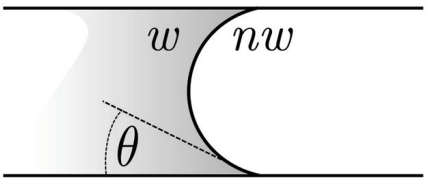

Figure 3.1: *Schematic diagram of two fluids of different wetting properties in a capillary tube. The colored gray area represents the wetting (w) and the white area is the non-wetting fluid (nw).*

Of course, fluids can be either wettable or non-wettable depending on the fluid they

are coupled with and the surface itself. As an example, when displacement of oil by water is studied in a glass Helle-Shaw cell. The water is going to be the wetting fluid. If the glass is replaced by a plexiglas cell then the roles of the water and oil in wetting the cell switch over. For the plexiglas cell the oil is the wetting fluid. This implies that when preparing experiments similar to those presented in the thesis, the choice of the materials from which the synthetic porous matrix is built and the choice of fluid pairs is critical. The situations when the materials and fluids are not picked with their wettability properties in mind can lead to the so-called mixed wettability. In the work presented here the fluid pairs and the materials are selected so that the effects of mixed wettability are avoided.

3.1 Physics of non-stimulated drainage

A flow process is characterized by an invading pattern. The invading pattern is formed as the defending is being displaced by the invading fluid. Generally the efficiency of the displacement and the morphological characteristics of the pattern are controlled by three sorts of forces. Keeping in mind that the focus here is on a quasi two-dimensional flow in the horizontal plane the gravity as a controlling force is excluded. The remaining two forces, capillary and viscous, and their relative strength is what categorizes the flow as capillary or viscous fingering [4].

When considering a drainage process in a porous medium the capillary forces act against the flow. The invading process starts when the imposed pressure difference between the present fluids is large enough to overcome the local capillary pressure thresholds. The capillary pressure is the pressure difference between the wetting and non-wetting fluid. It depends on the pore geometry expressed by the principal radii of curvature R_1 and R_2 and the interfacial surface tension γ. The capillary pressure is given by Young-Laplace law

$$p_c = p_{nw} - p_w = \gamma(\frac{1}{R_1} + \frac{1}{R_2})\,. \tag{3.1}$$

The capillary pressure threshold is the capillary pressure at the narrowest part of the pore throat. In the experiments the typical pore space is of size a, and the capillary pressure threshold is approximated by $p_t \approx 2\gamma/a$.

The velocity at which the fluid moves through the medium is dependent on the model's permeability (κ), the viscosity of the wetting fluid itself (η_w) and the viscous pressure gradient (∇p). The functional relationship of these quantities is summarized in Darcy's law

$$\mathbf{v} = -\frac{\kappa}{\eta_w}\nabla p\,. \tag{3.2}$$

Darcy's velocity ($\mathbf{v}$) is also known as seepage or filtration velocity.

Driving drainage processes at different velocities results in different flow regimes. Those flow regimes results in the invading clusters that feature distinctive morphological characteristics. To characterize the flow regimes usually a set of or a single dimensionless number is used. In studying non-stimulated drainage capillary number (Ca) and viscosity ratio (M) are commonly used dimensionless numbers [4].

Capillary number can be defined in many ways. Here, we define capillary number as the ratio of the viscous and capillary pressure drop over the same pore

$$\mathrm{Ca} = \frac{\Delta p}{p_c} = \frac{\eta_w v a^2}{\gamma \kappa} \,. \tag{3.3}$$

Another number that is useful in characterizing the flow regimes is the viscosity ratio between the fluid pairs ($M = \eta_{nw}/\eta_w$). By tuning these two numbers a wide array of different flow patterns can be achieved. For example in a slow ($\mathrm{Ca} \ll 1$) horizontal displacement of a more viscous wetting by a less viscous non-wetting fluid, the flow is going to be dominated by the capillary force effects and the invading structure is going to be characterized by the capillary fingering morphology. The capillary fingering geometry is well reproduced by the invasion percolation (IP) algorithm [5, 6, 7, 8, 9].

For the same fluid pair driven at higher speeds ($\mathrm{Ca} \gg 1$), the flow is governed by the viscous forces. In this case the invasion of the fluid that is more viscous than the defending fluid ($M \gg 1$), results in a stable displacement [10, 8, 11]. A fast displacement of the more viscous fluid by the less viscous one gives viscous fingering [12, 13, 8, 14]. The viscous fingering invading patterns are similar to those achieved in diffusion limited aggregation (DLA) (see [15, 13, 8]). The two presented scenarios represent the most extreme cases.

However, when $M \ll 1$ for a range of intermediate outflow velocities the flow is dominated by the capillary forces on a smaller scale and the viscous forces on the larger scale. Consequently, the invading patterns created in an intermediate regime demonstrate characteristics of both, capillary and viscous fingering depending on the spatial scale at which they are studied [16]. The critical spatial length-scale between the regimes is defined as $l_c = a/\mathrm{Ca}$ [16, 14]. The invading structure patterns on the scales lesser than l_c exhibit the characteristics of the capillary fingering while on the scales larger than l_c the invading clusters closely resemble a viscous fingering pattern. This finding is particularly important and is more thoroughly described in the first paper presented in the thesis.

Even though the experiments presented in the thesis are performed in the horizontal plane it is worth of mentioning that in a non-horizontal system, gravity and density contrast between the fluids become important factors. In a non-horizontal displacement tuning those two parameters in addition to M and Ca results in a variety of displacement structures [17, 18, 19, 20].

In this segment a brief overview of the growth of the invading cluster is addressed. In the carried out experiments the flow is characterized with low values of Ca ($\propto 10^{-4}$

and lower) and $M < 1$. Driving the invasion slowly the effects of the viscous forces are minimized and the front invades the largest pores first since they exert the least resistance. The interfacial pressure builds up until the easiest pore is invaded. The invasion is not limited to only one pore and it lasts as long as the pressure difference in the advancing part of the interface is large enough to overcome the capillary thresholds in the neighboring pores. The growth process is apparently not continuous [21, 22, 23, 24] and is characterized by so called *bursts* or Haines jumps. After a burst the pressure in the invading fluid builds up again until it is large enough to overcome the capillary pressure barrier in another pore throat along the front. A typical example of an invading pattern created in the capillary regime is shown in Figure 3.2

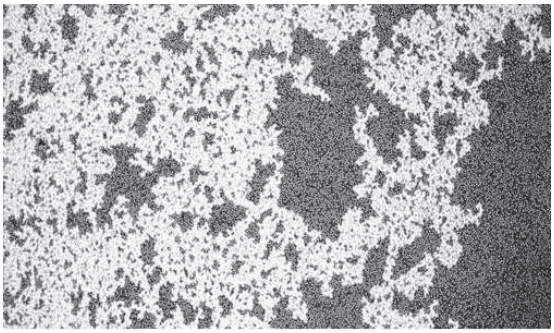

Figure 3.2: *Typical morphology of an invading structure created in the capillary fingering regime. The direction of the displacement is from the left hand side to the right hand side of the image.*

3.2 Physics of a seismically stimulated drainage process

While the unperturbed flow is very well understood there has been relatively a few studies that investigate impact of different sorts of stimulation applied to the flow in porous materials. Stimulated flows are actually of significant practical importance. The interest in seismically stimulated flow of immiscible fluids has been becoming increasingly popular since the latest reports on the enhanced oil recovery that followed seismic events [1, 2]. The methods used to stimulate oil recovery vary. They range from the use of surfactants to reduce the surface tension between the phases in the reservoir [25, 26] to the use of elastic waves in the mobilization of trapped oil bubbles [1, 27, 28, 29, 30] .

This thesis mainly deals with seismically stimulated drainage. Two out of three papers presented in the thesis address the flow that is seismically stimulated. The stimulation of the flow is performed in two ways. Those two approaches are different and their effect on the physics of the flow are discussed separately.

When the flow is stimulated by means of the oscillating pressure in the non-wetting phase, the elasticity of the porous matrix plays an important role. The model elasticity and its effects on the physics of the flow are addressed first.

In the case of the vibrational stimulation the hydrostatic pressure build up due to the arising body force in the wetting phase has a considerable impact on the growth of the invading cluster. The oscillatory hydrostatic pressure locally changes the invasion probability of the pores on the interface, which largely affects the growth of the invading cluster and its morphology. This effect is present in both, the longitudinal and transversal stimulation.

3.2.1 Pressure skin-depth in an elastic, two-dimensional porous medium

A seismic wave consists of two components, the S- and P- wave. When a seismic stimulation is applied to a porous system (e.g. rock) the S-wave corresponds to a shear wave of a rock matrix and does not propagate through fluids since there is no shear stress in fluids. The P-wave is also known as the compressional component of a seismic wave. In a porous material the soft inclusions increase the elasticity of the system. Usually the soft part of the matrix is the air pockets either in the rock matrix itself or in the present fluids. The compressional component of the seismic wave (P-wave) affects the softer part of the matrix. Applying a large scale homogeneous compression on a system with soft inclusions creates a large stress variation around the soft inclusions. The trapped air amplifies the amplitude of the imposed creating even a larger oscillation than that caused by the P-wave. According to Biot's theory [31, 32] this amplified oscillation emits secondary waves that propagate through the surrounding medium as a diffusion wave. This situation is closely reproduced by employing pressure oscillations on the non-wetting phase. Some of the effects of the pressure oscillations on the non-wetting phase in a slow drainage process are shown in Figure 3.3.

When the oscillatory method is applied a huge role in what can be observed in the behavior of the fluid flow is due to the elastic properties of the model. Due to the elasticity of the porous matrix within each oscillatory cycle its volume changes. As opposed to a stiffer system where the pressure oscillations propagate through the entire system, here those oscillations are attenuated over a certain length. This skin-depth can be estimated. Assuming that the wetting fluid is incompressible ($\rho_w = const.$), the permeability (κ) of the model is constant and considering the spatial variation of the height negligibly small when compared to the model thickness h_0 the time derivative of the non-wetting fluid pressure can be expressed as

$$\partial_t p = D\nabla^2 p, \tag{3.4}$$

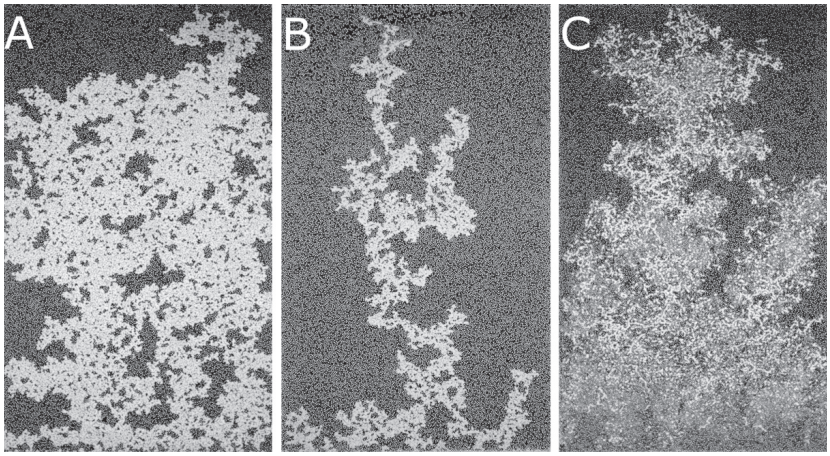

Figure 3.3: *Examples of breakthrough images of the invading cluster created in a drainage process stimulated with the oscillating pressure. The applied frequency is 0.2* Hz and the amplitudes of the oscillating component vary. The structures shown on the images A, B and C are created at 20, 560 and 3700 Pa, respectively. The outflow rate of the wetting fluid is Q=0.022 ml/min. The dark area on the images represents the wetting fluid while the white area is the invading air cluster.

where the diffusion constant is

$$D = \frac{\kappa p_{\mathrm{atm}}}{\eta_w \phi_0 \xi} \,. \tag{3.5}$$

The ξ term is the measured elasticity coefficient of the model. Considering the one-dimensional case (invariance in the transverse direction; i.e. $p{=}p(x,t)$), the pressure skin depth in the direction of flow (x) can be calculated by solving Eq. (3.4). The boundary condition on the inlet is $p(0) = P\cos(\omega t) + p_{\mathrm{atm}}$, where P and $\omega = 2\pi f$ are the amplitude and angular frequency of the applied oscillation. On the outlet, we assume $\nabla p_\infty = -v_0 \eta_w / \kappa$. Now, the real part of

$$p = P e^{i(kx-\omega t)} + p_{\mathrm{atm}} \,, \tag{3.6}$$

gives the solution for $p(x,t)$ where the wave number is

$$k = \frac{\sqrt{2}}{2}(1+i)\sqrt{\frac{\omega \eta_w \phi_0 \xi}{p_{\mathrm{atm}} \kappa}} \,. \tag{3.7}$$

The imaginary part of k gives the damping and the length ahead of the front over which the pressure is reduced by $1/e$ (skin-depth) is

$$x_s = \frac{1}{\mathrm{Im}\; k} = \sqrt{\frac{2 p_{\mathrm{atm}} \kappa}{\omega \eta_w \phi_0 \xi}} \,. \tag{3.8}$$

This pressure skin-depth depends on the frequency of the oscillations. The effects of the damping of the pressure oscillations caused by the elasticity of the synthetic porous medium are shown in Figure 3.4. A full derivation of the skin-depth dependency on the

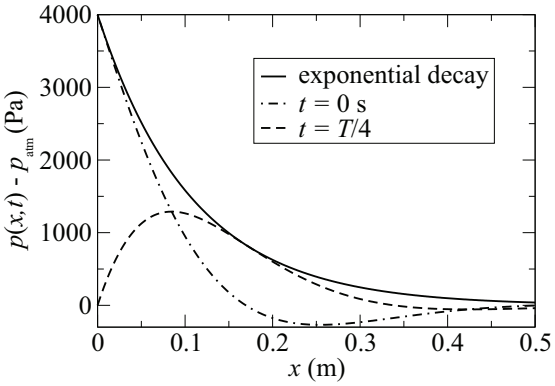

Figure 3.4: *Pressure wave propagation in the defending fluid as a function of the distance ahead of the invasion front. The dash-dot line represents the decay of the pressure amplitude with distance at time* $t = 0$*, the dashed line represents the pressure decay with distance at* $t = T/4$ *(*$T = 1/f$*)and the solid line represents the exponential decay of the pressure oscillation amplitude(envelope). The initial amplitude of the oscillation is 4000* Pa and the frequency is 0.2 Hz.

frequency and the amplitude of the oscillations is described in greater detail in paper no. 2, where the effects of the oscillatory pressure on the flow pattern geometry are addressed.

Due to the elasticity of the porous model the front moves back and forth within an oscillatory cycle. The back and forth traveling distance depends on the intensity and the frequency of the applied pressure oscillation. For the high frequency cases these lengths were considerably smaller than the ones observed in the low frequency experiments. In the cases when the incursion distance is considerably larger than the typical pore size the invasion cluster gets fragmented. In the extreme cases formation of foam is observed. The likeliness of fragmentation is then defined as a ratio of the backwards traveling distance (Δx^-) and the pore size (a)

$$F = \frac{\Delta x^-}{a}. \tag{3.9}$$

This dimensionless number is called fragmentation number. The backward traveling distance can be estimated as a product of the time scale of the oscillations and an approximation of the velocity of the menisci

$$\Delta x^- \approx \frac{1}{\omega}\frac{\kappa P}{\eta_w x_s}. \tag{3.10}$$

Finally in the case when the pressure oscillations are employed to simulate seismic activity F reads

$$F = \frac{1}{\omega}\frac{\kappa P}{\eta_w x_s a} = \sqrt{\frac{P^2 \kappa \phi_0 \xi}{4\pi f \eta_w p_{\mathrm{atm}} a^2}} = c\frac{P}{\sqrt{f}}. \tag{3.11}$$

and is proportional to the pressure oscillation amplitude and inversely proportional to the square root of the frequency. When the model and fluid characteristic parameters (i.e. elasticity coefficient, permeability, pore size, porosity, viscosity) are held constant as it was case in the experiments, then $c = 5.7 \cdot 10^{-5}$ ($\mathrm{Pa}^{-1}\mathrm{s}^{-1/2}$) in Eq. 3.11.

As a reality check we look at the elastic properties of a real reservoir rock saturated with water. Applying Biot's [31] theory of pressure wave propagation in a fluid-saturated porous material, the pressure propagation in this scenario can be described by a diffusion equation with the diffusion coefficient D_r [32]. Considering that the major contribution to the elasticity of the system originates from the soft inclusions (fluid and trapped air bubbles) the diffusion coefficient can be represented with

$$D_r = \frac{\kappa_r}{\beta\eta}, \tag{3.12}$$

where κ_r is the permeability of the porous medium, β is the compressibility and η is the viscosity of the soft medium. Analogously to our quasi-two dimensional case the fragmentation number for a real, three-dimensional porous material can be calculated as:

$$F = \frac{\kappa_r P}{a\eta\sqrt{2D_r\omega}}\ . \tag{3.13}$$

In an artificially induced moderate seismic event with the pressure amplitude $P = 10^3$ Pa and frequency of 1 Hz [33], water compressibility $\beta = 10^{-10}$ Pa^{-1}, and the permeability of the solid matrix $\kappa_r = 10^{-11}$ m^2 with pore sizes of 10^{-5} m, the calculated value of F (see Eq. 3.13) is 0.07. This value is on par with the values calculated in the experiments which confirms the high fidelity of our representation of a real world porous medium (see Paper 2 in the thesis).

3.2.2 Effects of the oscillating body force

When the porous matrix is exposed to the vibrational stimulation of the acceleration amplitude A and frequency f the menisci on the interface between the phases oscillate. The oscillations of the menisci are due to the arising body force in the referent frame of the porous matrix

$$F_b = A\rho_w e^{i\omega t}, \tag{3.14}$$

where $\omega = 2\pi f$ is the angular frequency and ρ_w is the wetting fluid density. The acceleration of the body force has the same magnitude as the imposed vibrations but the opposite orientation.

As a result of the arising body force there is a hydrostatic pressure build up in the fluid. The hydrostatic pressure changes the invasion probability of the pores on the front. The easiest way to describe the effects of the oscillatory hydrostatic pressure is to look at the system stimulated in the direction of the flow and at two pores, α and β of approximately the same size on a frontal instability.

In Figure 3.5, pores α and β are separated the distance Δx in the direction of the

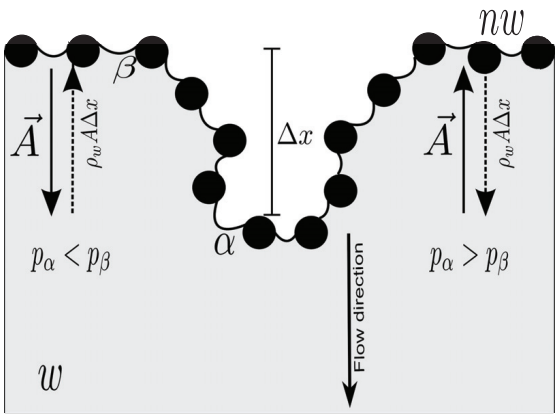

Figure 3.5: *Schematic diagram of the oscillatory hydrostatic pressure build up on a frontal instability. The wetting phase is represented by the gray area and marked $'w'$. The non-wetting phase is marked $'nw'$. The acceleration of the system is given by $\vec{A}$. The solid line arrows point in the direction of the system acceleration. The dashed arrows represent the generated hydrostatic gradient for the corresponding acceleration. The disks along the front represent the solid parts of the porous matrix. For the reason of a better legibility only the matrix solids along the front are shown.*

background flow. The body force acting on the fluid creates the hydrostatic pressure gradient $\Delta p_{\alpha\beta} = \rho_w A\Delta x$. The direction of the hydrostatic pressure gradient is always oriented opposite to the acceleration of the system. When the system is accelerated in the direction of the flow due to $\Delta p_{\alpha\beta} = \rho_w A\Delta x$ the fluid pressure in the proximity of pore α is lower than that around pore β therefore the invasion probability of pore α is larger. Analogously, pore β is more likely to be invaded on the other side of the oscillatory cycle, when the system acceleration is opposing the background flow. Depending on the orientation of $\Delta p_{\alpha\beta} = \rho_w A\Delta x$ the front is going to be either destabilized or stabilized. The growth around pore α has the destabilizing effect and the growth of the displacing cluster around pore β tends to stabilize the front.

When studying the system exposed to the vibrational stimulation we see a notable change in the invading cluster geometry as compared to those achieved in the same system without the external stimulation. Both, the stimulation in the direction of the

flow and in the direction perpendicular to it have large effects on the invading cluster geometry.

When the vibrational stimulation is applied the invading cluster geometry changes depending on the oscillatory frequency and the acceleration amplitude. A few examples of the effects of the oscillatory stimulation applied in the direction of the flow for different values of the frequency and amplitude are shown in Figure 3.6.

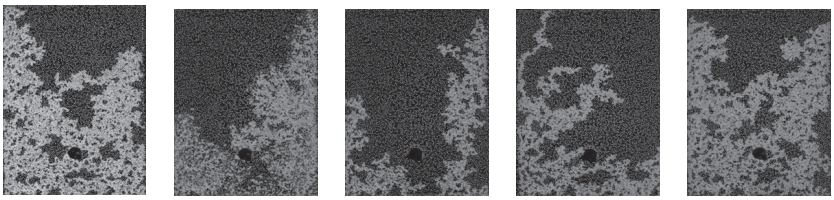

Figure 3.6: *Examples of invading cluster geometries achieved for the longitudinal vibrations of different amplitudes* A (m/s^2) and frequencies f(Hz).

The transversal vibrational stimulation of the porous system creates the hydrostatic gradient that acts along the system width. In this case, the sides of the porous matrix are always more probable to be invaded than the middle section. This leads to the finger-like geometries of the invading cluster in which the fingers grow along the sides of the model (Figure 3.7).

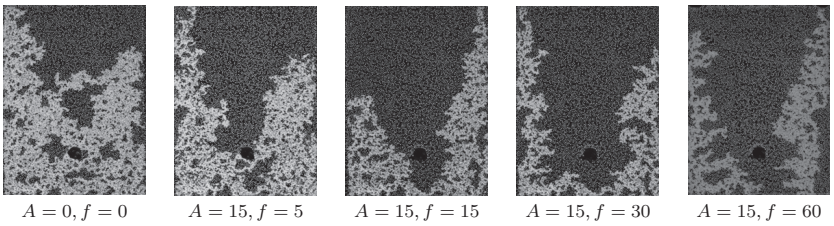

Figure 3.7: *Examples of invading cluster geometries achieved for the transversal vibrations of different amplitudes* A (m/s^2) and frequencies f (Hz).

To confirm the observed results in both, the transversal and longitudinal case, we resort to the numerical simulations of invasion-percolation (IP). The very well known IP algorithm [7, 8, 9] is modified to include the effects of the oscillatory hydrostatic pressure gradient [34, 35, 36]. In the case when the effects of the longitudinal acceleration are included the capillary pressure threshold in a pore with coordinates (x, y) is

$$p_t(x, y) = N(x, y) + (-1)^s A_{IP} x. \tag{3.15}$$

The term $N(x, y)$ represents the invasion probability of the site without any stimulation and is a random number uniformly distributed between 0 and 1. In the longitudinal case, terms A_{IP} and x are the oscillatory amplitude and the position of the pore from the model inlet, respectively. The s term represents the invasion step and as shown in Eq. 3.15 will change the orientation of the pressure gradient after each successive invasion. In the transversally imposed oscillations, the x term represents the position relative to the matrix side walls. The simulations are performed on a system of 400×600 lattice sites. As seen from Figure 3.8 and Figure 3.9, the numerical results in both, the longitudinal and transversal, are in agreement with the experimental results.

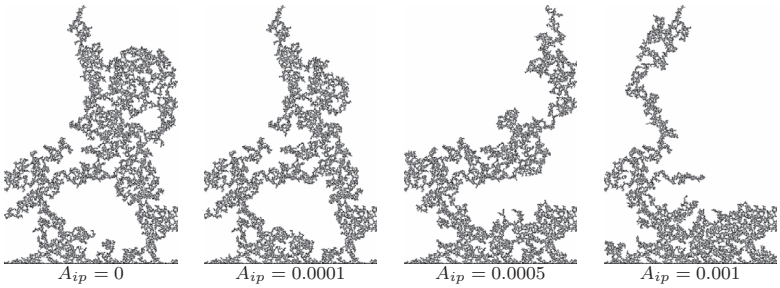

Figure 3.8: *Breakthrough images from the modified IP simulation for select values of A_{ip}. The gradient is applied in the direction of the flow. The black areas represent the non-wetting fluid and the white area is the wetting phase.*

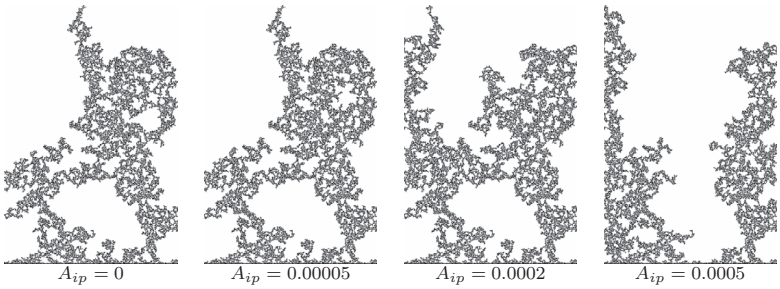

Figure 3.9: *Breakthrough images from the modified IP simulation for select values of the oscillatory acceleration A_{ip}. The gradient is applied in the direction perpendicular to the flow direction. The black areas represent the non-wetting fluid and the white area is the wetting phase.*

4 Introduction to the scientific papers

The thesis consists of three scientific articles. The author of the thesis is also the first author on two articles (Paper2 and Paper3). The author contributes to the first article (Paper 1) in terms of laboratory work. The laboratory work embraces preparations of and performing experiments and collection of the data from the measurements.

The articles included are integrated in the body of the dissertation in a logical order. As a courtesy to the less experienced reader we try to introduce the problem of the non-stimulated drainage first. We believe that getting acquainted with the general postulates of drainage makes a great introduction to the rest of the thesis. The following two articles deal with modifications of two phase drainage.

4.1 Paper 1

The first paper presents the effects of viscous forces on dynamic saturation–pressure curves. A series of drainage experiments is performed on a synthetic porous model. The porous cell is transparent so that the geometry of the evolving invading cluster can be monitored and recorded. The flow is driven either by slowly increasing the hydrostatic pressure difference between the fluid in the porous matrix and an externally placed open container or by a slow removal of the wetting fluid using a syringe pump. The amount of extracted and injected fluid during an experiment is measured and plotted as a function of the measured pressure in the wetting phase. The results from the quasi-static experiments exhibit notable differences when compared to the standard water-retention curves. It is shown that the dynamic effects reported in the literature are a combined effect of the capillary pressure oscillation along the front and the viscous forces. By combining detailed information on the invading cluster geometry with the measured pressure, capillary number and saturation we propose a scaling relation that connects pressure, saturation and the capillary number. This scaling relation might be of importance in reservoir modeling.

4.2 Paper 2

The second paper addresses the effects of oscillatory pressure on a slow flow of two immiscible fluids in an elastic synthetic porous medium. As the defending fluid (wetting phase) is displaced a pressure oscillation is applied to the invader (non-wetting phase). The displacement as well as the amplitude and the frequency of the oscillatory stimulation are kept constant throughout an experiment. The withdrawal speed of the wetting fluid is kept low forcing the background flow to stay in the capillary regime. The geometry of the invading cluster is investigated. It is found that the resulting morphology of the invader is dependent on the elasticity of the porous system, the amplitude and the frequency of the applied pressure oscillation. Different combinations of the amplitudes and frequencies result in morphologically similar geometries. To classify the characteristic structures of the invader a dimensionless number is proposed and successfully used.

4.3 Paper 3

The third paper shows the consequences of the vibrational stimulation on the morphology of the invading cluster generated in a slow drainage process. The wetting fluid is slowly removed letting the non-wetting fluid advance and create an invasion pattern. In each experiment the vibrational parameters are kept fixed. The direction of the vibrational stimulation is also fixed in individual experiments. The experiments are performed with the stimulation acting in the direction and perpendicular to the direction of the background flow. When the flow is stimulated in the direction of the flow, the resulting invading cluster geometries change as the vibrational acceleration and frequency change. The change in the invading cluster morphology reflects in the saturation of the matrix with the non-wetting fluid S_{nw}. It is found that S_{nw} scales very well with the amplitude to frequency A/f ratio. In the case of the transversal stimulation a notable lack of frequency dependency is present. The saturation data scale with the oscillatory amplitude A. It is also found that the gravity field that arises as a response to the imposed system acceleration and the corresponding hydrostatic pressure build up have a great impact on the shape of the evolving invading cluster geometry.

Bibliography

[1] Igor A. Beresnev and Paul A. Johnson. Elastic-wave stimulation of oil production: A review of methods and results. *Geophysics*, 59:1000–1017, 1994.

[2] I. A. Beresnev, R. D. Vigil, W. Q. Li, W. D. Pennington, R. M. Turpening, P. P. Iassonov, and R. P. Ewing. Elastic waves push organic fluids from reservoir rock. *Geophys. Res. Lett.*, 32:L13303, 2005.

[3] S. M. Hassanizadeh, M. A. Celia, and H. K. Dahle. Dynamic effect in the capillary pressure–saturation relationship and its impacts on unsaturated flow. *Vadose Zone Journal*, 1:38–57, 2002.

[4] R. Lenormand, C. Zarcone, and A. Sarr. Mechanisms of the displacement of one fluid by another in a network of capillary ducts. *Journal of Fluid Mechanics*, 135:337–353, 1983.

[5] R. Chandler, J. Koplik, K. Lerman, and J. F. Willemsen. Capillary displacement and percolation in porous media. *Journal of Fluid Mechanics*, 119:249–267, 1982.

[6] D. Wilkinson and J. F. Willemsen. Invasion percolation: a new form of percolation theory. *Journal of Physics A: Mathematical and General*, 16:3365–3376, 1983.

[7] R. Lenormand and C. Zarcone. Invasion percolation in an etched network: measurement of a fractal dimension. *Physical Review Letters*, 54:2226–2229, 1985.

[8] R. Lenormand, E. Touboul, and C. Zarcone. Numerical models and experiments on immiscible displacement in porous media. *Journal of Fluid Mechanics*, 189:165–187, 1988.

[9] R. Lenormand and C. Zarcone. Capillary fingering: Percolation and fractal dimension. *Transport in Porous Media*, 4:599–612, 1989.

[10] F. A. L. Dullien. *Porous Media Fluid Transport and Pore Structure*. Academic Press, San Diego, 1992.

[11] E. Aker, K. J. Måløy, and A. Hansen. Viscous stabilization of 2d drainage displacements with trapping. *Physical Review Letters*, 84:4589–4592, 2000.

[12] P. G. Saffman and G. Taylor. The penetration of a fluid into a porous medium or helle-shaw cell containing a more viscous fluid. *Proc. Roy. Soc.*, A245:312–329, 1958.

[13] Knut Jørgen Måløy, Jens Feder, and Torstein Jøssang. Viscous fingering fractals in porous media. *Physical Review Letters*, 55:2688–2691, 1985.

[14] G. Løvoll, Y. Méheust, R. Toussaint, J. Schmittbuhl, and K. J. Måløy. Growth activity during fingering in a porous hele-shaw cell. *Physical Review E*, 70:026301, 2004.

[15] T. A. Witten and L. M. Sander. Diffusion-limited aggregation, a kinetic critical phenomenon. *Physical Review Letters*, 47:1400–1403, 1981.

[16] R. Toussaint, G. Løvoll, Y. Méheust, K. J. Måløy, and J. Schmittbuhl. Influence of pore-scale disorder on viscous fingering during drainage. *Europhysics Letters*, 71:583–589, 2005.

[17] D. Wilkinson. Percolation model of immiscible displacement in the presence of buoyancy forces. *Physical Review A*, 30:520–531, 1984.

[18] A. Birovljev, L. Furuberg, J. Feder, T. Jøssang, K. J. Måløy, and A. Aharony. Gravity invasion percolation in 2 dimensions - experiment and simulation. *Physical Review Letters*, 67:584–587, 1991.

[19] G. Wagner, A. Birovljev, P. Meakin, J. Feder, and T. Jøssang. Fragmentation and migration of invasion percolation clusters: Experiments and simulations. *Physical Review E*, 55:7015–7029, 1997.

[20] Y. Méheust, G. Løvoll, K. J. Måløy, and J. Schmittbuhl. Interface scaling in a two-dimensional porous medium under combined viscous, gravity and capillary effects. *Physical Review E*, 66:051603, 2002.

[21] W. B. Haines. Studies in the physical properties of soil. v. the hysteresis effect in capillary properties, and the modes of moisture distribution associated therewith. *J. Agr. Sci.*, 20:97–116, 1930.

[22] Norman R. Morrow. Physics and thermodynamics of capillary action in porous media. *Industrial and Engineering Chemistry*, 62:32–56, 1970.

[23] K. J. Måløy, L. Furuberg, J. Feder, and T. Jøssang. Dynamics of slow drainage in porous-media. *Physical Review Letters*, 68:2161–2164, 1992.

[24] L. Furuberg, K. J. Måløy, and J. Feder. Intermittent behavior in slow drainage. *Physical Review E*, 53:966–977, 1996.

[25] John C. Fountain, Andrew Klimek, Michael G, Beikirch, and Thomas M. Middleton. The use of surfactants for in situ extraction of organic pollutants from a contaminated aquifer. *Journal of Hazardous Materials*, 28:295–311, 1991.

[26] Kurt D. Pennell, Min Quan Jin, Linda M. Abriola, and Gary A. Pope. Surfactant enhanced remediation of soil columns contaminated by residual tetrachloroethylene. *Journal of Contaminant Hydrology*, 16:35–53, 1994.

[27] Lakshmi N. Reddi and Sreedhar Challa. Vibratory mobilization of immiscible liquid ganglia in sands. *Journal of Environmental Engineering*, 120:1170–1190, 1994.

[28] Peter M. Roberts, Igor B. Esipov, and Ernest L. Majer. Elastic-wave stimulation of oil reservoirs: Promising eor technology? *The Leading Edge*, 22:448–453, 2003.

[29] Markus Hilpert. Capillarity-induced resonance of blobs in porous media: Analytical solutions, lattice-boltzmann modeling, and blob mobilization. *Journal of Colloid and Interface Science*, 309:493–504, 2007.

[30] S. R. Pride, E. G. Flekkøy, and O. Aursjø. Seismic stimulation for enhanced oil recovery. *Geophysics*, 73:023–035, 2008.

[31] M. A. Biot. Mechanics of deformation and acoustic propagation in porous media. *Journal of Applied Physics*, 33:1482–1498, 1962.

[32] S. R. Pride. *'Relationship between seismic and hydrological properties' in Hydrogeophysics, edited by Rubin Y. and Hubard S. S.* Springer Netherlands, 2005.

[33] P. M. Shearer. *Introduction to seismology*. Cambridge University Press, 1999.

[34] A. Birovljev, L. Furuberg, J. Feder, T. Jssang, K. J. Mly, and A. Aharony. Gravity invasion percolation in two dimensions: Experiment and simulation. *Phys. Rev. Lett.*, 67(5):584–587, Jul 1991.

[35] Paul Meakin, Jens Feder, Vidar Frette, and Torstein Jo/ssang. Invasion percolation in a destabilizing gradient. *Phys. Rev. A*, 46(6):3357–3368, Sep 1992.

[36] M. Chaouche, N. Rakotomalala, D. Salin, B. Xu, and Y. C. Yortsos. Invasion percolation in a hydrostatic or permeability gradient: Experiments and simulations. *Phys. Rev. E*, 49(5):4133–4139, May 1994.

I

This article is removed.

II

This article is removed.

III

This article is removed.